ARCHIVES OF METALLURGY AND MATERIALS
Volume 60 2015 Issue 2
DOI: 10.1515/amm-2015-0223

A. WIENGMOON*,♯, P. SUKCHOT*, N. TAREELAP**, J.T.H. PEARCE***, T. CHAIRUANGSRI****

EFFECTS OF T6 HEAT TREATMENT WITH DOUBLE SOLUTION TREATMENT ON MICROSTRUCTURE, HARDNESS AND CORROSION RESISTANCE OF CAST Al-Si-Cu ALLOY

WPŁYW OBRÓBKI TERMICZNEJ T6 POŁĄCZONEJ Z PODWÓJNYM PRZESYCANIEM NA MIKROSTRUKTURĘ, TWARDOŚĆ ORAZ ODPORNOŚĆ NA KOROZJĘ STOPU Al-Si-Cu

Effects of T6 heat treatment with double solution treatment on microstructure, hardness and corrosion resistance of a cast A319 (Al-4.93wt%Si-3.47wt%Cu) alloy were investigated. The T6 heat treatment comprised of the first solution treatment at 500±5°C for 8 h, the second solution treatment in the temperature range of 510 to 530±5°C for 2 h followed by water quenching (80°C), and artificial aging at 170°C for 24 h followed by water quenching (80°C). Microstructure of the alloy was studied by optical microscopy and electron microscopy, Rockwell hardness was measured, and corrosion resistance in 0.1 M NaCl aqueous solution was determined by a potentiodynamic technique. The results revealed that the T6 heat treatment with double solution treatment led to an improvement in corrosion resistance and comparable macrohardness as compared to those obtained from the case of single solution treatment. The second solution treatment at 520°C is the optimum leading to relatively low corrosion current density without substantial drawbacks on breakdown potential or the width of passive range.

Keywords: Al-Si-Cu alloy, heat treatment, age hardening, microstructure, hardness, corrosion resistance

W pracy badano wpływ obróbki termicznej T6 połączonej z podwójnym przesycaniem na mikrostrukturę, twardość oraz odporność na korozję stopu A316 (Al-4,93Si-3,47Cu w % wag.) otrzymanego metodą odlewania. Obróbkę termiczną T6 przeprowadzono w następujący sposób: w pierwszej kolejności stop poddano przesycaniu w temperaturze 500±5°C przez 8 godzin, a następnie w zakresie temperatur od 510 do 530±5°C przez 2 godziny, hartowanie wodą (80°C) oraz sztuczne starzenie w 170°C przez 24 godziny i ponowne hartowanie wodą (80°C). Mikrostrukturę stopu badano metodami mikroskopii optycznej i mikroskopii elektronowej. Pomiar twardości stopu wykonano metodą Rockwella. Odporność stopu na korozję w roztworze wodnym 0.1 M NaCl wyznaczono metodą potencjodynamiczną. Otrzymane wyniki wykazały, że obróbka termiczna T6 z podwójnym przesycaniem prowadzi do poprawy makrotwardości oraz odporności materiału na korozję w porównaniu do stopu poddanego pojedynczemu przesycaniu. Stwierdzono także, iż drugie przesycanie w temperaturze 520°C jest optymalne i prowadzi do stosunkowo niskiej gęstości prądu korozyjnego bez znaczących odchyleń potencjału rozkładowego lub szerokości zakresu pasywnego.

1. Introduction

Because of its excellent castability, corrosion resistance and high strength-to-weight ratio, cast Al-Si-Cu (A319) alloys are commonly used as cylinder blocks, cylinder heads, pistons, valve lifters and crankcases for internal combustion engines in automotive industry [1,2]. The alloys contain Fe and Mn as impurities and various microstructural phases have been found, including eutectic (acicular) Si and intermetallic phases such as θ-(Al_2Cu), Mg_2Si, π-($Al_8Mg_3FeSi_6$), α-($Al_{15}(Mn,Fe)_3Si_2$) and β-(Al_5FeSi) [3]. The A319 alloys are heat treatable using artificial aging and their strengthening is usually through precipitation hardening by θ'-Al_2Cu and Mg_2Si [2]. The tensile properties and ductility of an A319 alloy were investigated in the as-cast condition, after solution treatment at 485°C (T4 treatment) for 4.5 h, and after solution treatment followed by aging at 230°C (T7 treatment) for 4.5 h [3], in which tensile testing was performed at the temperature range from -90 to 400°C. It was noted [3] that bulk precipitate coarsening coupled with alloy softening mechanisms become active and dominant at temperatures above 300°C. Some additional elements can be added to modify A319 alloys to improve their mechanical properties. Small amount of Zr was added as the rate-controlling element to resist coarsening of Al_3Zr precipitates due to low diffusivity and solubility of zirconium in aluminium and low energy precipitate/matrix interfaces, so that thermal stability and hence hardness and wear resistance of the Zr-modified alloy can be improved [2]. The base alloy and the Zr-modified alloy were subjected to T6 treatment comprising of solution treatment at about 500°C, quenching

---

[*] DEPARTMENT OF PHYSICS, FACULTY OF SCIENCE, NARESUAN UNIVERSITY, PHITSANULOK, 65000, THAILAND
[**] SCHOOL OF ENERGY, ENVIRONMENT AND MATERIALS, KING MONGKUT'S UNIVERSITY OF TECHNOLOGY THONBURI, BANGKOK, 10140, THAILAND
[***] PANYAPIWAT INSTITUTE OF MANAGEMENT, NONTHABURI, 11120, THAILAND
[****] DEPARTMENT OF INDUSTRIAL CHEMISTRY, FACULTY OF SCIENCE, CHIANG MAI UNIVERSITY, CHIANG MAI, 50202, THAILAND
[♯] Corresponding author: ampornw@nu.ac.th

in water at room temperature and artificial aging treatment in the temperature range of 175 to 235°C. It has been reported that the highest hardness levels of both alloys were obtained at the aging temperature of 175°C [2]. Effects of Sr addition, cooling rate and the T6 treatment on the hardness of an A319 alloy have also been studied [4]. Recently, effects of the T6 treatment (solution treatment at 500°C for 8 h, quenching in hot water at 80°C, and aging at 150 to 230°C for 1-48 h) on hardness and tensile strength of an A319 alloy were reported, in which the peak hardness and the maximum tensile strength was obtained by aging at 170°C for 24 h [5]. By using HRTEM and HAADF-STEM, the precipitates at peak aging of this A319 alloy have been identified predominantly as coherent θ''-(Al$_3$Cu) together with a minority of semi-coherent θ'-(Al$_2$Cu) [6].

Even though single-stage solution treatment at a temperature below 495°C is the normal heat treatment for the A319 alloys, it has been recognized that a single solution treatment of the A319 alloy could not lead to a complete dissolution of Cu-containing particles e.g. at 485°C for 4.5 h [3]. Consequently, efforts have been made to use a higher solution temperature [7] and a double solution treatment [8,9] in order to substantially dissolve Cu-containing intermetallic compounds. Haro et al., 2009 [7] recommended the solution temperature of 504°C for 8 h followed by water quenching (60°C) plus aging at low temperature of 154°C for 6 h to obtain improved mechanical properties of the A319 alloy. An increase in the solutionizing temperature from 504 to 545°C was recommendable only for short solutionizing time of 4 h, and an increase in the aging temperature from 154 to 200°C led to improved hardness but at the expense of decrease in ductility. Sokolowski et al., 1995 [8] recommended a double solution treatment at 495°C for 8 h and then at 520°C for 2 h followed by water quenching (70°C) plus artificially aging at 250°C for 5 hours, which gave rise to improved homogenization and superior mechanical properties (strength, elongation and impact). Panagopoulos et al. 2009 [9] used T6 heat treatment with double solution treatment at 495°C for 2 h and then at 515°C for 4 h followed by water quenching plus artificial aging at 250°C for 3 h, which can improve corrosion resistance of the treated alloy in a strong alkaline solution of 0.1 M NaCl adjusted to pH>12 by concentrated NaOH. Accordingly, the optimum condition of T6 heat treatment with double solution treatment for the A319 alloy is not in full agreement. Moreover, the aging temperature of the T6 treatment used in the previous works using double solution treatment [8,9] was above 200°C, which is relatively high as compared to the optimum aging temperature reported in some other works, e.g. 175°C [2], 170°C [5] or 154°C [7].

In the present study, effects of the T6 heat treatment on microstructure, hardness and corrosion resistance of cast Al-Si-Cu (A319) alloy were therefore studied by aiming to use solutionizing temperature higher than 495°C with double solution treatment and relatively low aging temperature below 200°C.

2. Experimental

2.1. Materials and heat treatment

An experimental alloy was prepared by melting a 30 kg charge in a graphite clay crucible in an electric furnace and superheating to a temperature of 800°C. The melt was degassed with high purity argon, and then poured at 730°C into a metal mould to produce tensile test bars according to the JIS standard. Chemical composition of the cast Al-Si-Cu alloy is given in TABLE 1. Single solution treatment was done at 500±5°C for 8 h followed by water quenching (80°C). To find the optimum condition for double solution treatment, the first solution treatment was done at 500±5°C for 8 h, whereas the second solution treatment was performed at different temperatures as 510, 520 or 530±5°C for a relatively short time of 2 h followed by water quenching (80°C). Artificial aging was performed at the optimum aging temperature previously reported [5], i.e. 170°C for 24 h followed by water quenching (80°C). The conditions for heat treatments of all specimens are summarized in TABLE 2.

TABLE 1

Chemical composition of cast Al-Si-Cu alloy [wt.%]

Si	Cu	Fe	Mg	Zn	Mn	Ni	Sn	Ti	Al
4.93	3.47	0.29	0.19	0.06	0.04	0.01	0.01	0.01	bal.

TABLE 2

Heat treatment conditions

Specimen symbol	Conditions of heat treatments					
	First solution treatment	Quenching	Second solution treatment	Quenching	Artificial Aging	Quenching
AC	-	-	-	-	-	-
S	500°C / 8 h	hot water (80°C)	-	-	-	-
S-A	500°C / 8 h	hot water (80°C)	-	-	170°C / 24 h	hot water (80°C)
SS10	500°C / 8 h	hot water (80°C)	510°C / 2 h	hot water (80°C)	-	-
SS20	500°C / 8 h	hot water (80°C)	520°C / 2 h	hot water (80°C)	-	-
SS30	500°C / 8 h	hot water (80°C)	530°C / 2 h	hot water (80°C)	-	-
SS10-A	500°C / 8 h	hot water (80°C)	510°C / 2 h	hot water (80°C)	170°C / 24 h	hot water (80°C)
SS20-A	500°C / 8 h	hot water (80°C)	520°C / 2 h	hot water (80°C)	170°C / 24 h	hot water (80°C)
SS30-A	500°C / 8 h	hot water (80°C)	530°C / 2 h	hot water (80°C)	170°C / 24 h	hot water (80°C)

2.2. Microstructural examination

Specimens were ground on silicon carbide papers down to 1000 grits, and then progressively polished with 1 and 0.3 μm Al_2O_3. The etchant used for optical microscopy (OM) and scanning electron microscopy (SEM) was 5 ml of HF in 100 ml in distilled water. The microstructure was studied using a LEO 1455LV scanning electron microscope equipped with an EDAX detector for energy dispersive X-ray spectroscopy (EDS). The volume fraction of phases in the microstructure was determined from area fraction in optical micrographs by the ImageJ software, based on 3-5 different areas.

2.3. Hardness measurement

Macrohardness testing was performed on un-etched specimens by a Rockwell hardness tester in the B scale (HRB) using a steel ball, 100 kgf load and 15 seconds indenting time. The mean value is based on ten different areas on each specimen.

2.4. Corrosion testing

Corrosion resistance was determined by a potentiodynamic technique over an area of 1 cm^2 on specimens using an ECO Chem, autolab model PGSTAT 30 potentiostat, a voltage increase rate of 20 mV/s, and 0.1 M NaCl aqueous solution as electrolyte at room temperature. A saturated Ag/AgCl electrode and a platinum counter electrode were used as a reference electrode and auxiliary electrode. The corrosion resistance was determined *via* an analysis of anodic polarisation characteristics in terms of passive current density, passive range and passivity breakdown potential. The corroded surfaces of the specimens subjected to T6 heat treatment with double solution treatment and their cross-sections were also investigated by SEM-EDS for understanding the relationship between their microstructure and corrosion behaviour.

3. Results and discussion

3.1. Microstructure

The microstructure of all specimens with different heat treatments was shown by optical micrographs in Fig. 1. In the as-cast condition (Fig. 1(a)), the microstructure consists of primary dendritic α-Al and interdendritic structure. Fig. 2 shows an optical micrograph at a higher magnification and a backscattered electron image (BEI) in SEM of interdendritic structure of the as-cast specimen. Corresponding SEM-EDS spectra from phases present in the as-cast specimen were also given in Fig. 2, from which α-Al (marked '1'), eutectic Si (marked '2') and intermetallics, including Al_2Cu (marked '3') and β-Al_5FeSi (marked '4') as previously reported by Rincon et al. [3], were revealed. However, π-($Al_8Mg_3FeSi_6$) or α-($Al_{15}(Mn,Fe)_3Si_2$) has not been observed in the present study due possibly to relatively low content of Mg and Mn in the experimental alloy. The Al_2Cu and β-Al_5FeSi intermetallics exhibit the brighter contrast in SEM-BEIs due to their relatively higher average atomic weight as compared to α-Al or eutectic Si. To recognize these interdendritic phases in optical micrographs, it can be noted that the eutectic Si appears black, whereas the intermetallics (Al_2Cu and Al_5FeSi) appear greyish after etching by aqueous HF solution.

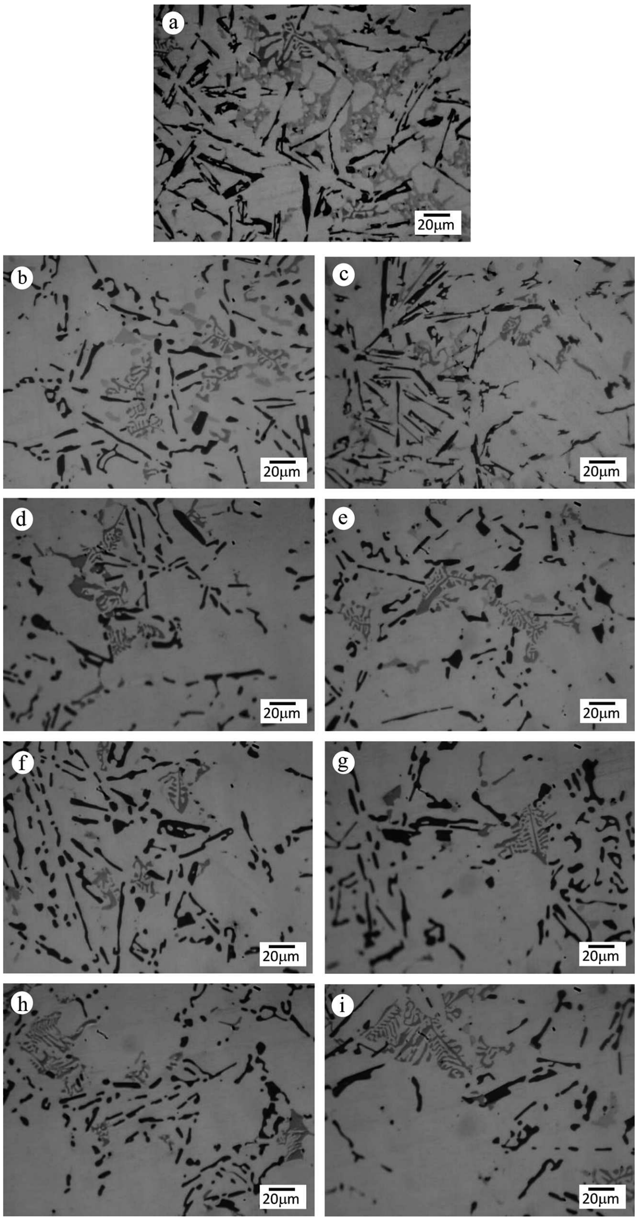

Fig. 1. Optical micrographs compare the microstructure and area fraction of interdendritic phases: (a) AC, (b) S, (c) S-A, (d) SS10, (e) SS10-A, (f) SS20, (g) SS20-A, (h) SS30 and (i) SS30-A, respectively

Table 3 shows the volume fraction of eutectic Si and intermetallics in the alloy specimens with different heat treatments. After single solution treatment (Fig. 1(b)), spheroidisation of the eutectic structure occurred and the amount of the eutectic structure was decreased as can be seen from the lower volume fraction of interdendritic phases in Table 3. This indicates that the single solution treatment applied can lead to some dissolution of interdendritic phases. Likewise, spheroidisation of the eutectic structure occurred after double solution treatment (see Figs. 1(d, f and h)). As expected, dissolution of interdendritic phases can be enhanced by double solution treatment applied as indicated from the lower volume fraction of interdendritic phases in Table 3 as compared to that in the case of single solution treatment. Hence, double solution treatment applied somewhat promoted dissolution of interdendritic phases. From Table 3, an increase in the temperature of the second solution treatment in the range of 510 to 530°C and the application of aging heat treatment did not significantly affect the change in volume fraction of interdendritic phases.

TABLE 3

Volume fractions of interdendritic phases (eutectic Si and intermetallics phases) present in the alloy specimens with different heat treatments

Specimen	Volume fraction of interdendritic phases (%)
AC	24.75
S	13.57
SS10	10.90
SS20	11.87
SS30	10.58
S-A	13.14
SS10-A	10.34
SS20-A	11.01
SS30-A	10.48

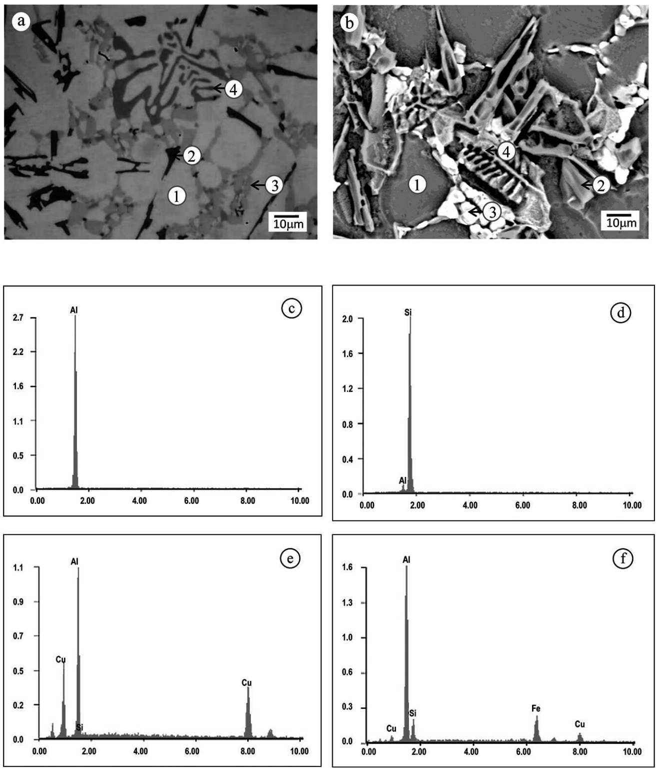

Fig. 2. (a) Optical micrograph and (b) SEM-BEI show the microstructure of the as-cast (AC) specimen. (c-f) Corresponding EDS spectra of α -Al (marked '1'), Si (marked '2'), Al_2 Cu (marked '3') and Al_5FeSi (marked '4'), respectively

The precipitates formed at 170°C for 24 h in the case of single solution treatment are mainly θ''-Al_3Cu and θ'-Al_2Cu, the details of which have been studied by transmission electron microscopy (TEM) and reported elsewhere [6]. For the cases of double solution treatment, it is presumed that the same types of precipitates were formed and are accountable for the improvement in the hardness of the experimental alloy.

3.2. Hardness measurement

The macrohardness of the specimens subjected to different heat treatments was shown in Fig. 3. After single or double solution treatment, the macrohardness was increased due to dissolution of intermetallic phases into the α-Al matrix leading to solid-solution strengthening. As compared to single solution treatment, double solution treatment applied without aging treatment can improve the alloy hardness for some extent, but the effect is not pronounced. This is reasonable considering a slight difference in the volume fraction of interdendritic phases in both cases, shown in TABLE 3. After aging treatment, the alloy hardness was effectively increased by precipitation hardening within the matrix as has been shown for example in Fig. 3. The maximum macrohardness (73 HRB) was obtained in the alloy specimen with single solution treatment plus aging at 170°C for 24 h (i.e. S-A in Table 2). This is not fully understood, but it could be due to the less volume fraction of interdendritic phases for the cases of double solution treatment. Moreover, the difference in the content of alloying elements in the α-Al matrix by single or double solution treatment possibly caused a difference in the rate of precipitation and hence the optimum peak aging time. Hence, further study on effects of single and double solution treatments on kinetics of aging precipitation in cast Al-Si-Cu alloy should be carried out.

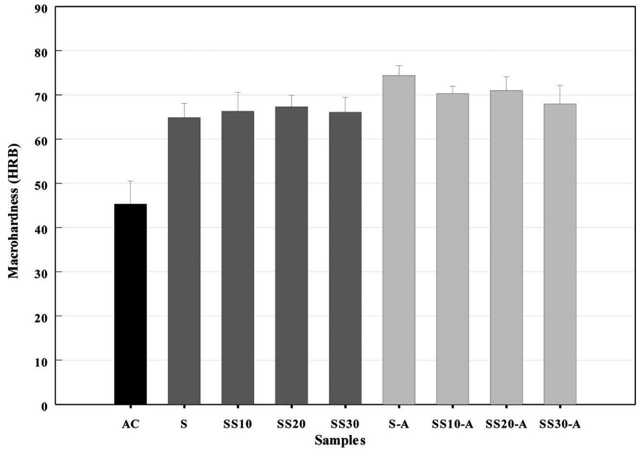

Fig. 3. Effects of different heat treatments on the macrohardness of the experimental alloy

3.3. Corrosion behaviour

The anodic polarisation curves are shown in Fig. 4 and corrosion data obtained from those curves are listed in TABLE 4. Passivation is exhibited in all alloy specimens subjected to different heat treatments. In general, all specimens subjected to solution and aging treatments possessed a wider passive range of the anodic polarisation curves than that of the as-cast specimen. Aging treatment led to a higher $I_{passive}$ as compared to the specimens subjected only to solution treatment, which can be attributed to a greater anodic activity at the matrix areas depleted in Al and Cu adjacent to cathodic Al_2Cu or Al_3Cu particles.

The beneficial effects of increasing temperature in the second solution treatment to 520-530°C are that the open circuit potential (OCP) is less negative and the I_{pass} is reduced, but the disadvantages are that the break-down potential ($E_{breakdown}$) is more negative and the width of passive range is narrower. Hence, it was considered that the second solution treatment at 520°C is the optimum leading to low I_{pass} without substantial drawbacks on the $E_{breakdown}$ or the width of the passive range. This optimum condition is comparable to that recommended by Sokolowski et al. [8] (double solution treatment at 495°C for 8 h and then at 520°C for 2 h followed by water quenching (70°C) plus artificially aging at 250°C for 5 h) for obtaining improved homogenization and superior mechanical properties of the A319 alloy. The important difference to point out is that a lower aging temperature at 170°C can be successfully applied in the present study for improving hardness and corrosion resistance of the A319 alloy.

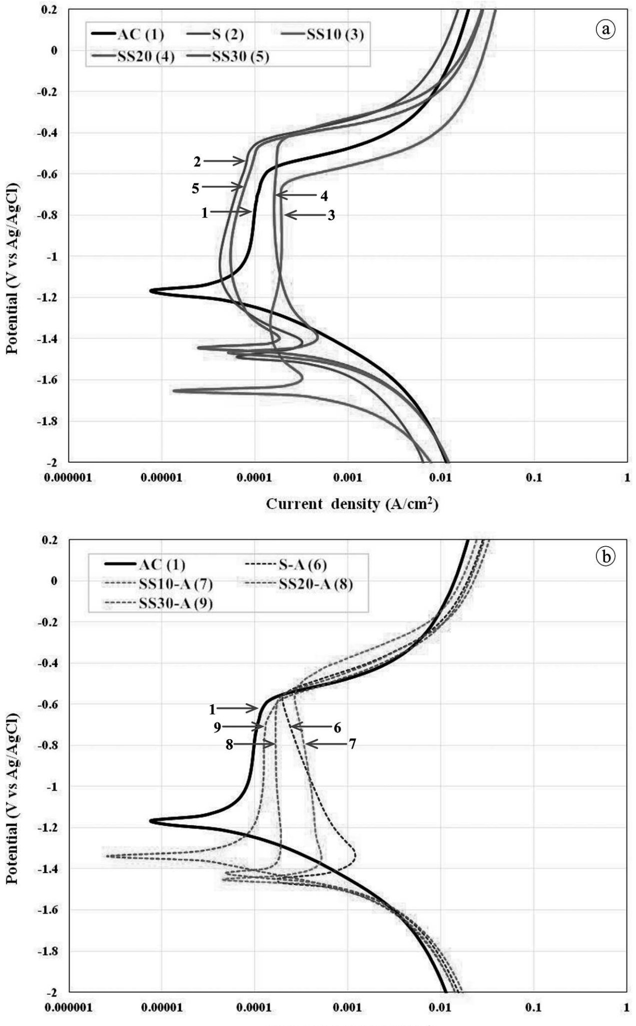

Fig. 4. Anodic polarisation curves of the specimens subjected to different heat treatments: (a) as-cast and solution treatment, (b) as-cast and solution treatment plus aging treatment

Fig. 5(a) shows a secondary electron image (SEI) in SEM representing the plan view of a corroded surface of the experimental alloy subjected to double solution treatment plus aging treatment. The SEM-EDS spectrum in Fig. 5(b) indicated that the corrosion products on the corroded surfaces after electrochemical polarization are mainly alumina (Al_2O_3) or aluminosilicates. Fig. 6(a) shows SEM-BEI of a cross section of corroded surface of the experimental alloy subjected to double solution treatment plus aging treatment, in which severe pitting attack on the α-Al matrix (anode) around Si eutectic phase (cathode) was observed. Cevik et al. [10] reported that corrosion progressed in the form of pitting which nucleates and proceeds around the Al_3Ti intermetallic in AA6063 alloy. The attack on the matrix can also lead to the removal of the intermetallic phases. This is in agreement to the observations by Panagopoulos et al. [9] and Son et al. [11]. The SEM-EDS spectrum in Fig. 6(b) indicated that some copper oxides are present together with alumina (Al_2O_3) or aluminosilicates as corrosion products within the pits. During the passivation range, the alumina layer may dissolve uniformly and pitting occurs in competition to re-passivation up to the $E_{breakdown}$. At the potential higher than the $E_{breakdown,}$ stable

TABLE 4

Data from corrosion testing by anodic polarization technique

Specimen	I_{pass} (mA/cm^2)	OCP (mV)	$E_{breakdown}$ (mV)	Passive range (mV)
AC	0.10	-1170	-600	570
S	0.04	-1490	-470	1020
SS10	0.16	-1650	-680	970
SS20	0.17	-1470	-450	1020
SS30	0.06	-1450	-470	980
S-A	0.95	-1450	-550	900
SS10-A	0.95	-1450	-510	940
SS20-A	0.18	-1420	-570	850
SS30-A	0.14	-1340	-600	740

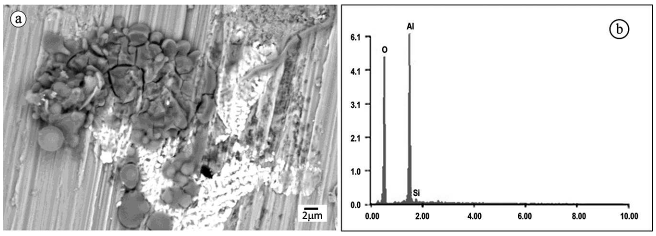

Fig. 5. (a) SEM-SEI, (b) SEM-EDS spectrum from the oxides on corroded surface of the SS10-A specimen after corrosion testing

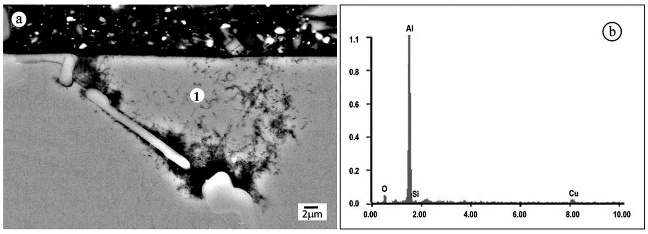

Fig. 6. (a) SEM-SEI, (b) SEM-EDS spectrum from the oxides on corroded surface of the SS10-A specimen after corrosion testing

growth of pits will be possible. In the presence of chloride ions [12,13] suggested that pitting of aluminium and aluminium alloys may be initiated by adsorption of chloride ions on weak spots in the oxide surface. Penetration of chloride ions through the oxide film is possible *via* vacancy transport and localized dissolution of aluminium at the metal/oxide interface finally occurred.

4. Conclusions

1. In the as-cast condition, the microstructure of the cast Al-4.93wt%Si-3.47wt%Cu alloy consists of primary dendritic α-Al and interdendritic phases, including eutectic Si, Al_2Cu and β-Al_5FeSi. Double solution treatment promoted dissolution of interdendritic phases. An increase in the temperature of the second solution treatment in the range of 510 to 530°C and the application of aging treatment did not significantly affect dissolution of interdendritic phases.

2. The macrohardness after T6 heat treatment was effectively increased by precipitation hardening within the matrix. The maximum macrohardness was obtained from the alloy specimen subjected to T6 heat treatment with single solution treatment, while that obtained from the alloy specimen subjected to T6 heat treatment with double solution treatment was comparable.

3. T6 heat treatment with double solution treatment led to an improvement of corrosion resistance of the alloy in 0.1 M aqueous NaCl solution as compared to that obtained from the case of single solution treatment. The second solution treatment at 520°C is the optimum leading to relatively low I_{pass} without substantial drawbacks on breakdown potential or the width of passive range. A relatively low aging temperature at 170°C can be successfully applied for improving hardness and corrosion resistance of the A319 alloy.

Received: 20 February 2014.

Acknowledgements

The authors would like to acknowledge Naresuan University for funding support. The authors gratefully thank the Science Lab Center, Faculty of Science, Naresuan University, for use of SEM facilities.

REFERENCES

[1] H. Chandler, ASM International, Materials Park, Heat Treater's Guide Practices and Procedures for Nonferrous Alloys, Materials Park, OH, 1996.

[2] R. Mahmudi, P. Sepehrband, H.M. Ghasemi, Mater. Letts. **60**, 2606-2610 (2006).

[3] E. Rincon, H.F. Lopez, M.M. Cisneros, H. Mancha, Mater. Sci. Eng. A **519**, 128-140 (2009).

[4] O. El Sebaie, A.M. Samuel, F.H. Samuel, H.W. Doty, Mat. Sci. Eng. A **486**, 241-252 (2008).

[5] A. Wiengmoon, P. Apichai, J.T.H. Pearce, T. Chairuangsri, Adv. Mater. Res. **770**, 88-91 (2013).

[6] A. Wiengmoon, J.T.H. Pearce, T. Chairuangsri, S. Isoda, H. Saito, H. Kurata, Micron, **45**, 32-36 (2013).

[7] S. Haro, J. Ramírez, D.K. Dwivedi, E. Martínez, Mater. Sci. Tech. **25**, 886-891 (2009).

[8] J.H. Sokolowski, X-C. Sun, G. Byczynski, D.O. Northwood, D.E. Penrod, R. Thomas, J. Mater. Process. Technol. **53**, 385-392 (1995).

[9] C.N. Panagopoulos, E.P. Georgiou, K.I. Giannakopoulos, Mater. Corros. **60**, 415-418 (2009).

[10] E. Cevik, Y. Sun, H. Ahlztci, Arch Metall Mater. **57**, 469-477 (2012).

[11] I.J. Son, H. Nakano, S. Oue, S. Kobayashi, H. Fukushima, Z. Horita, Mater. Trans. **49**, 2648-2655 (2008).

[12] E. McCafferty, Corros. Sci. **37**, 481-492 (1995).

[13] M. Chiba, Y. Nakayama, T. Hiraga, H. Takahashi, Y. Shibata, Surf. Interface Anal. **45**, 1626-1630 (2013).